UPPSALA
UNIVERSITET

K11004

Examensarbete 30 hp
Februari 2011

Nanostructured Cathodes

-A step on the path towards a fully interdigitated 3-D microbattery

David Rehnlund

UPPSALA
UNIVERSITET

Teknisk- naturvetenskaplig fakultet
UTH-enheten

Besöksadress:
Ångströmlaboratoriet
Lägerhyddsvägen 1
Hus 4, Plan 0

Postadress:
Box 536
751 21 Uppsala

Telefon:
018 – 471 30 03

Telefax:
018 – 471 30 00

Hemsida:
http://www.teknat.uu.se/student

Abstract

Nanostructured Cathodes -A step on the path towards a fully interdigitated 3-D microbattery

David Rehnlund

The Li-ion field of battery research has in the latest decades made substantial progress and is seen to be the most promising battery technology due to the high volume and specific energy densities of Li-ionbatteries. However, in order to achieve a battery capable of competing with the energy density of a combustion engine, further research into new electrode materials is required. As the cathode materials are the limiting factor in terms of capacity, this is the main area in need of further research. The introduction of 3-D electrodes brought new hope as the ion transport path is decreased as well as an increased electrodearea leading to an increased capacity. This thesis work has focused on the development of aluminium 3-D current collectors in order to improve the electrode area and shorten the Li-ion transport path. By using a template assisted electrodeposition technique, nanorods of controlled magnitude and order can be synthesized. Furthermore, the electrodeposition brings excellent possibilities of upscaling for future industrial manufacturing of the batterycells. A polycarbonate template material which showed interesting properties, was used in the electrodeposition of aluminium nanorods. As the template pores were nonhomogeneously ordered a number of nonordered nanorods were expected to arise during the deposition. However,a surplus of nanorods in reference to the template pores was acquired. This behavior was investigated and a hypothesis was formed as to the mechanism of the nanorod formation. In order to achieve a complete cathode electrode, a coating of an ion host material on the nanorods is needed. Due to its high capacity and voltage, vanadium oxide was selected. Based on previous work with electrodeposition of V2O5 on platinum, a series of experiments were performed to mimic the deposition on an aluminium sample. Unfortunately, the deposition was unsuccessful as the experimental conditions resulted in aluminium corrosion which in turn made deposition of the cathode material impossible. The pH dependence of the deposition was evaluated and the conclusion was drawn, that electrodeposition of vanadium oxide on aluminium is not possible using this approach.

Handledare: Leif Nyholm
Ämnesgranskare: Torbjörn Gustafsson
Examinator: Karin Larsson
ISSN: 1650-8297, UPTEC K11004

1 Sammanfattning

Li-jonbatteriforskningen har de senaste decennierna gjort stora framsteg och Li-jonbatterier anses vara den mest lovande batteritekniken på grund av dess stora volym- och specifika energitäthet. Den explosiva utvecklingen av mikrosystem (väldigt små sensorer och robotar) har medfört ett stort behov av energikällor som kan skalas ned till några mikrometer. Li-jonbatterier har stor potential men för att ta steget till mikrovärlden krävs att energimängden/area förbättras. Lika som man i början av 1900-talet började bygga skyskrapor när invånartätheten ökade, så ser man även i batterivärlden till den tredje dimensionen. Genom att bygga 3-D batterier erhåller man en ökad mängd energi per area då jonerna har en större yta att reagera med.

Detta examensarbete har gått ut på att undersöka möjligheten att växa nanotrådar av aluminium för att vidare lägga på en film av aktivt Li-jonelektrodmaterial. Eftersom katod materialen är de begränsande i dagens batterier har fokus lagts på att utveckla dessa. Genom att använda poröst plastmembran har nanotrådar växt till lika dimensioner och homogen täckning. Det observerades att vid deponering erhålls fler trådar än det finns porer i membranet vilket tyder på någon sorts utökning av porerna under deponeringen. Detta mycket intressanta fenomen har undersökts och en hypotes kring dess ursprung har formulerats.

Contents

2 Introduction

2.1 The Li-ion Battery

With the ever growing concern for the planets health and the climate change, the need for high-power hybrid and electric vehicles has intensified. Finding high energy density batteries to power these vehicles has become a key issue in the further development of this technology. Additionally, the increased use of portable electronic devices has elevated the demands on batteries and especially their size, energy-density and efficiency. Compared to other available energy storage systems, Li-ion batteries have become the system of choice due to their low weight, high energy density and efficiency [1].

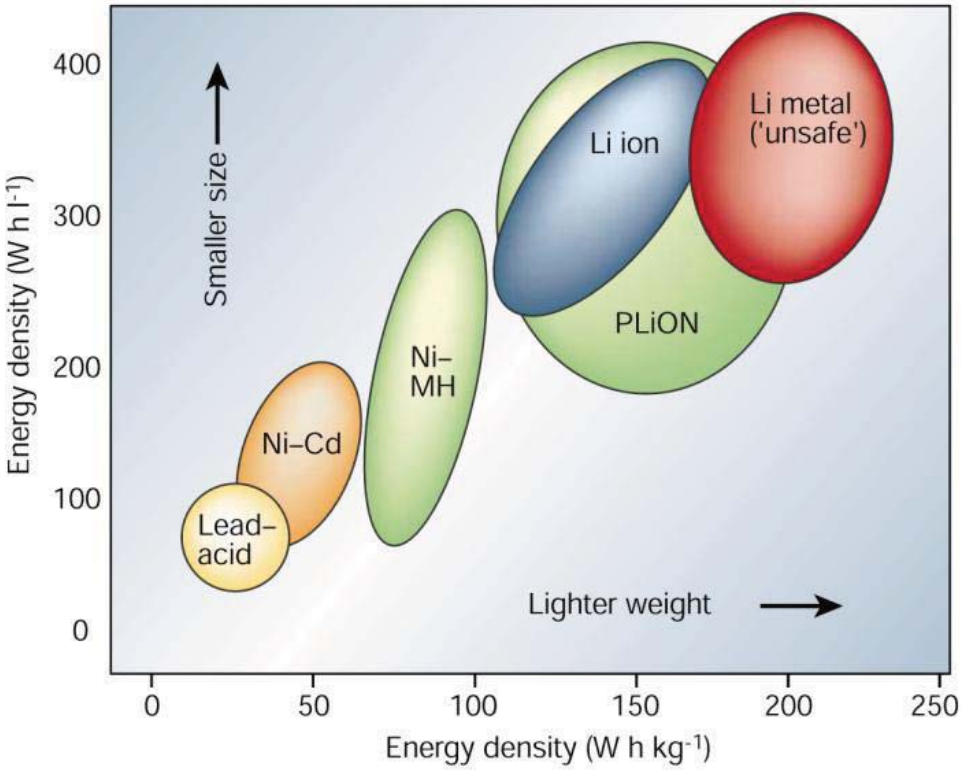

Figure 1: Comparison of energy density for different battery systems [1]

A cell is the basic electrochemical unit in a battery, providing electrical energy by converting chemical energy. A cell consist of two electrodes (an anode and a cathode) separated by a separator soaked in an electrolytic solution of conducting ions. As the Li-ion battery is cycled, Li^+ ions move back and forth between the anode and cathode, which has given the battery the appellation "rocking-chair" battery. Early studies revealed that the use of metallic lithium as anode leads to the formation of dendrites upon cycling,

which in turn may lead to short circuits and possible explosion risk. This started the search for new, more stable anode materials [2]. Currently the most common anode material is graphite, which stores lithium ions in its layered structure. With the intercalation potential of Li^+ into graphite so close to the reduction potential of Li^+ to Li metal, there is a risk of deposition of lithium metal on the anode upon cycling [3]. Graphite also suffers a capacity loss due to a necessary formation of a SEI (solid electrolyte interphase) layer [4]. Consequently new material research is prompted. Compounds known to alloy with lithium such as Al, Sn, Sb and Si are under investigation as potential anode materials mainly due to their high capacity to store lithium. However, the lithium inter-/deintercalation induced stress on the structures has shifted the focus to metal oxides and composite matrices which allow some structural support for the lithium ions movement. Among the many promising compounds, Cu_2Sb stands out with almost double the theoretical capacity of graphite [5].

As far as cathodes go, $LiCoO_2$ is the most common material, used in most commercial Li-ion rechargeable batteries. High cost and the toxicity of Co has lead to further investigations of alternative materials. Oxides of manganese and vanadium are good alternatives. Unlike the cobalt-based compounds, $LiFePO_4$ is inexpensive, nontoxic and very stable both chemically and thermally and therefore a prime candidate for the next generations cathode material [6]. Li_2FeSiO_4 is another prime alternative with similar qualities as $LiFePO_4$ [7].

2.2 Three-Dimensional Micro Batteries

The continued advance of micro electromechanical systems (MEMS) for optical, chemical and mechanical sensors and actuators has resulted in a wide range of autonomous devices. The fast expansion of MEMS systems has created a great demand for suitable power sources. Batteries can serve this purpose but, in order to be downscaled for MEMS applications, a reduction of their areal footprint must be accommodated. This creates a problem for the traditional two-dimensional batteries as the energy stored is proportional to the electrode area [6]. With that in mind, a new field of batteries has recently risen which focus on expanding the surfaces in the third dimension, thus increasing the battery performance without expanding the areal footprint. The increased electrode area allows a higher quantity of active material to be coated on the current collector which results in a higher energy density. The area gain also allows a higher amount of active material to come in contact with the electrolyte thus improving the ion transportation rate. The ion transportation path is further decreased by assembling the cathode and anode in specific geometries seen in Figure 2. These geometries have been constructed in order to maximize energy and power density [6]. The general idea is to limit the transportation path of the ions by assem-

bling the anodes and cathodes close together. This can be accomplished by constructing a cell with the following geometries: (a) arrays of interdigitated cylindrical electrodes, (b) interdigitated cathode and anode plates, (c) rod arrays of cylindrical anodes coated with a thin layer of electrolyte with the remaining volume filled with the cathode material, (d) aperiodic sponge architectures in which the solid network of the sponge serves as the charge-insertion cathode, which is coated with an ultra thin layer of electrolyte, and the remaining volume is filled with an interpenetrating continuous anode [6]. The structures described above are illustrated in Figure 2.

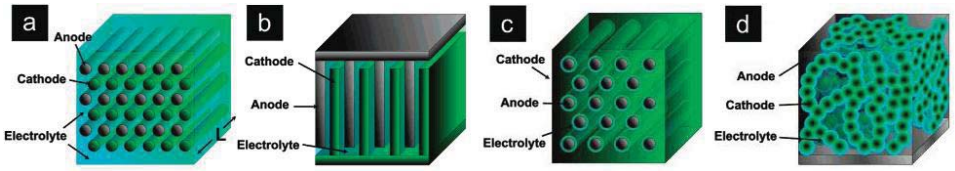

Figure 2: Geometrical structures of 3-D battery cells [6]

In addition to the high surface area, the 3-D electrodes can be composed of nanoparticles which have unique qualities. The particles enable: intercalation of ions without destroying the electrode material structure thus improving the cycle life, an increased insertion/removal rate for the ions due to the short transportation distance within the particles [3] as well as a short path length for the electronic transport (allowing materials with low electronic conductivity to be accessible) [8]. The large surface area also allows a large contact area for the electrolyte which in turn creates a high lithium-ion flux over the electrodes [3].

2.3 Aluminium nanorods

The field of nanosystems, such as nanowires and nanorods, has recently received a great deal of attention, especially for construction of 3-D microbatteries [9]. The most common approach to construct 3-D microbatteries is by using interdigitated rods as electrodes. In order to construct viable nanostructures for this application, free standing nanorods are required. As the resistance increase with the length of the nanorods, there is a natural limitation to the growth of the nanorods by electrochemical methods [10]. There are numerous methods available to synthesize nanorods, including vapor-liquid-solid (VLS) and template based deposition [11, 12]. Template based deposition is however the most versatile method, offering a variety of different nanostructures and synthesis of vastly different materials. Electrochemical template based deposition is a very popular method to synthesize nanostructures, mainly due to the possibility of industrial up-scaling. Porous polycarbonate (PC) and anodic aluminum oxide (AAO) membranes are often used as templates, mainly due to their commercial availability,

easy synthesis and with that undemanding replicability [12]. In fact, several research groups have recently started electrodepositing metals in PC membranes [13, 14, 15]. Al-nanorods can be electrodeposited on an aluminium substrate by using voltage pulse electrodeposition, as shown by Perre *et al.* [16]. This technique enables the synthesis of free standing Al-nanorods with different geometrical parameters according to the template geometry. Earlier, Taberna et. al synthesized copper nanorods onto copper substrates by template assisted electrodeposition [17]. As copper is oxidized at the high potentials used in Li-ion battery cathodes, it is advantageous to use aluminium as the cathode current collector [10].

The low standard potential of aluminium (E° = -1.67 V vs normal hydrogen electrode) makes electrodeposition in an aqueous media impossible, as the reduction of water occurs at a higher potential than aluminium [18]. Investigations into non-aqueous electrolytes resulted in the usage of organic solutions such as aromatic hydrocarbons and ethers. However their narrow electrochemical potential window and low electrical conductivity limited their applications. Further development in ionic liquids has given researchers a new alternative for the electrodeposition of aluminium. Among the many candidates are 1-ethyl-3-methylimidazolium chloride ([EMIm]Cl) which has shown to be the most promising liquid, mainly due to its wide electrochemical potential window, relative high conductivity and very low vapor pressure.

When preparing the ionic liquid, [EMIm]Cl must be mixed with aluminium chloride ($AlCl_3$). The molar ratio $AlCl_3$/[EMIm]Cl controls the deposition conditions. A ratio lower than 1 generates a high concentration of $AlCl_4^-$ resulting in a Lewis basic liquid. A ratio above 1 results in the formation of $Al_2Cl_7^-$ ions leading to a Lewis acidic ionic liquid. As the organic cation ($[EMIm]^+$) is reduced at more negative potentials than the dominant $AlCl_4^-$ ions in basic ionic liquid, aluminium cannot be deposited in basic ionic liquids. In the acidic ionic liquid, the reduction occurs as described in equation 1 [19].

$$4Al_2Cl_7^- + 3e^- \rightarrow Al + 7AlCl_4^- \tag{1}$$

Hence a molar ratio above 1 is needed to carry out the electrodeposition of aluminium in [EMIm]Cl ionic liquid.

2.4 Cathode Materials

The cathode material in a secondary lithium battery is a host for lithium ions. In order to have a high-quality cathode material the compound must be able to reversibly incorporate a large quantity of ions without significant structural changes. Furthermore, a high conductivity is required both for electrons and lithium ions. Finally the material must be of acceptable cost, meaning preparation of inexpensive materials in a low cost process [20].

The basic concept of a cathode material is the redox reaction of the transition metal as lithium ions are inserted and removed from the structure. Charge neutrality has to be maintained within the material as the ions are injected. However, the structure strain of compositional changes often leads to phase changes. This requires the use of stable structured materials over a wide range of compositions. The rate at which lithium ions are transported in and out of the material, as well as the access to ions near the electrode, controls the maximum discharge current.

For the past two decades $LiCoO_2$ has been the commercially most used material. However, the high cost of cobalt combined with the moderate specific capacitance has lead the research for alternative cathode materials. The main candidates are oxides of the transition metals Ni, Mn and V [21]. Recently $LiFePO_4$ has emerged as another strong candidate, mainly due to its low cost and stability [22]. Ever since Whittingham discovered that vanadium pentoxide can reversibly intercalate lithium it has been considered to be one of the most promising material for Li-ion battery cathodes [23]. Because vanadium has a wide range of oxidation states from +2 to +5, it separates itself from Co, Mn and Fe based cathodes which only accommodate one-electron transfer processes. This prime difference sets vanadium oxide (VO_x) apart in terms of high-energy density materials. Apart from a high capacity, VO_x also exhibits excellent cyclability where, for instance, Ding *et al.* showed a capacity of 142.5 mAh/g after 500 cycles (with an initial capacity of 160 mAh/g) [24]. The low electric conductivity and slow lithium ion diffusion in vanadium oxide has been pointed out as a problem for its use as a cathode material [20]. By using a current collector with a three dimensional structure and coating it with a thin layer of VO_x, this problem can however be tackled. The thin layer enables an increased lithium ion diffusion rate as well as enhanced electrical conductivity by using the higher conductivity of the underlying current collector [25].

2.5 Objective

The aim of this thesis is the development of nanostructured electrodes for 3-D battery applications. Based on template-assisted electrodeposition of nanostructured Al-current collector, the goal is to grow a field of Al-nanopillars, coat them with a suitable cathode material and finally assemble with an opposite 3-D anode electrode. The main focus will be on the characterization of the growth mechanisms of the Al-nanopillars and its effect on the template membrane.

3 Experimental procedures

3.1 Synthesis

The deposition of aluminium nanorods followed the work of Oltean *et al.* [26]. The coating of the nanorods with vanadium oxide was performed as described by Potiron *et al.* [27].

3.1.1 Preparation of Aluminium nanorods

In order to prevent unwanted reactions between the ionic liquid and the atmospheric water, a controlled atmosphere was used. An argon filled glove-box (with $[O_2]$ and $[H_2O] \leq 2ppm$) was used to limit the oxygen and water exposure to the samples. All synthesis steps containing the ionic liquid were therefore performed in a glove-box.

Preparation of the ionic liquid was done by carefully adding aluminium chloride powder (anhydrous powder, 99.99%, Sigma-Aldrich) into 1-ethyl-3-methylimidazolium chloride (98,5%, Fluka) during continuous stirring. For optimum result a $AlCl_3$:[EMIm]Cl molar ratio of 2:1 was used. Since the reaction between the two compounds is highly exotermic, the addition of $AlCl_3$ to [EMIm]Cl was carried out very slowly. A light white smoke was visible if the addition was too fast. The end product was a brown liquid.

3.1.2 Reduction of Al_2O_3

Before reducing the aluminium samples, the plates were immersed in a solution of 25 vol% H_2SO_4 (98%), 70 vol% H_3PO_4 (85%) and 5 vol% HNO_3 (52.5%) for 2 minutes. After rinsing with deionized water, the samples were degreased in an ethanol beaker placed in an ultrasonic bath for 15 minutes.

Before every nanorod deposition, the aluminium samples were first reduced in order to remove the thin layer of additives and aluminium oxide on the surface. A three-electrode setup connected to a potentiostat/galvanostat Autolab PGSTAT30 was used for the reduction. All electrodes were 1 cm x 1 cm aluminium plates. The setup was then immersed in the ionic liquid previously described. The reduction of the working electrode was performed for two samples which were later used as working and counter electrodes in a two-electrode setup.

3.1.3 Current pulse deposition

The deposition of aluminium nanorods followed the work of Oltean *et al.* [26]. The electrodeposition was carried out in a two-electrode setup connected to the same Autolab as described in section 3.1.2. The pretreated aluminium plates were used as counter and working electrodes. A PC porous membrane (in some experiments a nonporous PC film was used), provided

by Goodfellow, was placed on the working electrode followed by a cellulose separator, both soaked in ionic liquid. The counter electrode was then placed on top and the setup was clamped together, connected to the Autolab and immersed in the ionic liquid.

In the majority of all experiments a nucleation pulse of -0.9 V was applied, for 0.5 s. The pulsed deposition was performed by applying a current of -5 mA for a duration of 0.2 s followed by a resting pulse of 0 A for 2 s. This procedure was repeated for the desired number of cycles. By varying the number of cycles, the aluminium-nanorod growth could be examined.

When the deposition was complete, the aluminium sample with the porous membrane attached to it was soaked in acetonitrile to dissolve the reactive ionic liquid. The PC membrane could then be removed by dissolving it in dichloromethane.

3.1.4 V_2O_5 thin layer deposition

The coating of the nanorods with vanadium oxide was performed as described by Potiron *et al.* [27]. The electrolyte was mixed by adding vanadylsulphate to deionized water with the final concentration of 0.1 M. In order to achieve the wanted V_2O_5 phase the pH had to be controlled which was achieved by careful addition of sulphuric acid and/or sodium hydroxide. To establish the parameters for the electrodeposition, cyclic voltammetry and chronopotentiometry was performed on the vanadylsulphate solution.

Galvanostatic electrodeposition was performed with a constant current of 1 mA for a few preset time intervals. The cell was composed of a platinum counter electrode, an Ag/AgCl reference electrode and an aluminium working electrode all immersed in the vanadylsulphate electrolyte and connected to a PGSTAT30 Autolab.

Calculation of the charge used in the electrodeposition enabled further calculations of the height and mass of the deposited film according to equations 2 and 3.

$$m = nM = \frac{QM}{zF} = \frac{itM}{zF} \tag{2}$$

$$h = \frac{m}{A\rho} \tag{3}$$

3.2 Characterization

In order to establish the parameters of the deposition on an aluminium substrate, an initial electrochemical analysis of the properties of vanadium oxide deposition was performed. Consequently cyclic voltammograms and chronopotentiograms were recorded on the vanadium oxide system by using a PGSTAT30 Autolab.

Analysis of the sample structure and morphology was performed with a LEO 1550 (Zeits) scanning electron microscopy (SEM).

3.2.1 Electrochemical cycling

Evaluation of the cycling properties of the vanadium oxide coated aluminium plates (both 2-D plates and 3-D plates with nanorods) were carried out in a Digatron battery testing system. The battery cells were assembled in a glove box with controlled oxygen and water levels. The vanadium oxide coated aluminium plates were assembled with a piece of lithium foil separated by a glass fiber separator soaked in 1M $LiPF_6$-EC-DEC 2:1 electrolyte (a lithium salt in a Ethylene carbonate-diethyl carbonate solvent). The setup was placed in a polymer coated aluminium bag and sealed under vacuum. The cells were cycled between 2 and 4 V (vs Li^+/Li) with an applied current determined by equations 4 and 5. The potential window was chosen based on earlier reported cycling data for V_2O_5 [27].

$$Q = \frac{i_{dep} t_{dep}}{z} \tag{4}$$

$$i_{cycling} = \frac{Q}{t_{cycling}} = \frac{i_{dep} t_{dep}}{z t_{cycling}} \tag{5}$$

These calculations are based on the assumption that the entire charge accumulated in the electrodeposition of V_2O_5 is consumed in the oxidation of VO^{2+}.

3.2.2 Scanning Electron Microscopy

Scanning electron microscopy (SEM) has become the researcher's choice for early characterization of materials. The wide magnification window of 10x up to 300 000x offers the user a detailed image of the surface down to a few nanometers. Instead of an optical beam as in a common microscope a focused electron beam is fired at the sample where the incoming electrons either react with the sample atoms and emit secondary electrons (SE) or reflect and return as primary electrons. The emitted electrons are detected and by scanning the beam over the surface a micrograph is obtained [28].

3.2.3 X-ray Diffraction

X-ray diffraction (XRD) is a nondestructive analytical technique providing information about the material's crystallographic structure, chemical composition and physical properties. The technique is based on measuring the intensity of scattered X-rays from the sample as a function of the incoming and scattered angle of the X-ray beam. These parameters combined with the wavelength of the beam can be used in Bragg's law (see equation 6) to

establish the cell parameters of the material and furthermore the correct phase.

$$n\lambda = 2dsin(\theta) \tag{6}$$

This technique can be used to analyze all elements, however the heavier elements show an increased intensity and are therefore easier to analyze. For the lightest elements a neutron radiation source is required in order to achieve sufficient intensity. XRD is used to analyze bulk materials as well as thin films with a lower limit of 50 Å. With a decreased thickness of the film comes a need for a more powerful X-ray source, which can be met by exposing the sample to synchrotron radiation i.e. [28].

3.2.4 Energy-Dispersive X-ray Spectroscopy

Energy-dispersive X-ray spectroscopy (EDS or EDX) is an analytical tool for chemical characterization or simply elemental analysis. The technique centers around the reaction between the incoming particles and emitted X-ray radiation. By detecting the ejected X-rays which have a unique energy for every element, a chemical characterization of the sample is possible. Since the most common particle used is the electron, the EDS system is often combined with a SEM leading to a versatile analysis tool. However there are some limitations to the technique, for instance it is only able to detect elements with atomic number four and above as well as a minimum of 0.1wt% is required for detection [28].

3.2.5 X-ray Photoelectron Spectroscopy

X-ray photoelectron spectroscopy (XPS) is a nondestructive surface sensitive analysis technique in which the binding energy of elements are analyzed by detection of emitted photoelectrons with specific elemental energy. XPS centers around the reaction of incoming X-rays and the excitation state that follows. A relaxation of this excitation state gives rise to emission of photoelectrons as to balance the energy difference between the states. The photoelectrons have a unique energy for every element as well as their surrounding leading to information about the binding energy within the compound. By measuring the binding energy of the surface elements further conclusions regarding the elemental composition, empirical formula, chemical and electronic state can be drawn.

XPS is able to identify all elements with an atomic number of three and above, furthermore all states of the compounds can be detected (solids, liquids and gases) which enables XPS to be a very applicable surface analysis tool. The analysis depth varies with the state of the compound, however for solids the depth is somewhere between 2-20 monolayers [28].

4 Results and discussion

4.1 Aluminium nanorod current collector

Synthesis of the aluminium nanorods was performed by pulsed galvanostatic deposition. This technique has proven advantageous [26] as the resting pulse enables diffusion of the ions to the working electrode and therefore benefits the nanorod growth. Early experiments showed that a cycle time of 5000-6000 cycles was required to achieve a homogeneous coverage of the sample, as can be seen in Figure 3a and 3b.

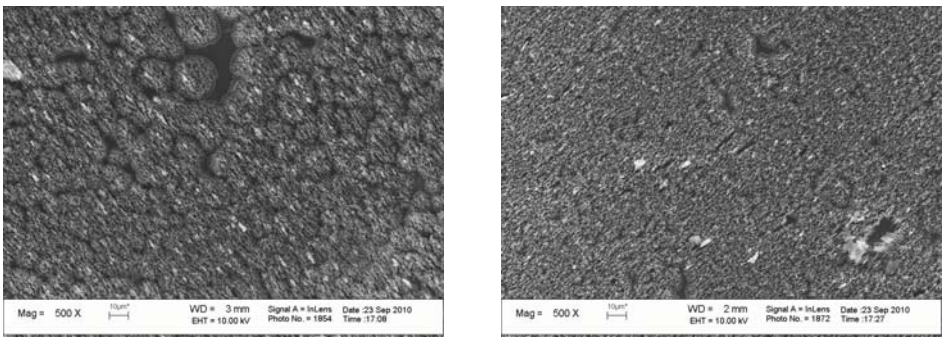

(a) 5000 cycle deposition (b) 6000 cycle deposition

Figure 3: Nanorod deposition at different cycles with a pulsed current of -5 mA (0.2 s)/0 A (2 s)

As proven by earlier research [26], a short nucleation pulse before the pulsed deposition improves the growth of nanorods. This result was verified by comparing samples with and without a pre-deposition nucleation pulse, as can be seen in Figure 4. By comparing the overall coverages of the samples, an advantage is noticeable with the nucleation pulse. Notice should also be taken to the height of the rods in Figure 4b compared to Figure 4a, where the height distribution among the rods is less consistent, which can be derived from the nucleation pulse. By implementing a nucleation pulse, the first step of nucleation which has a higher energy barrier, is facilitated and the continued nanorod growth is therefore assisted. This leads to an overall more homogeneous height of the nanorods.

4.1.1 Spontaneous nanorod growth

All aluminium electrodepositions were performed with a polycarbonate (PC) membrane with inhomogeneously ordered pores. This fact leads one to imagine that the nanorods would be arranged in the same way. However, by comparing SEM micrographs of the PC membrane and micrographs of the aluminium sample after deposition, it is clear that there was an excess of

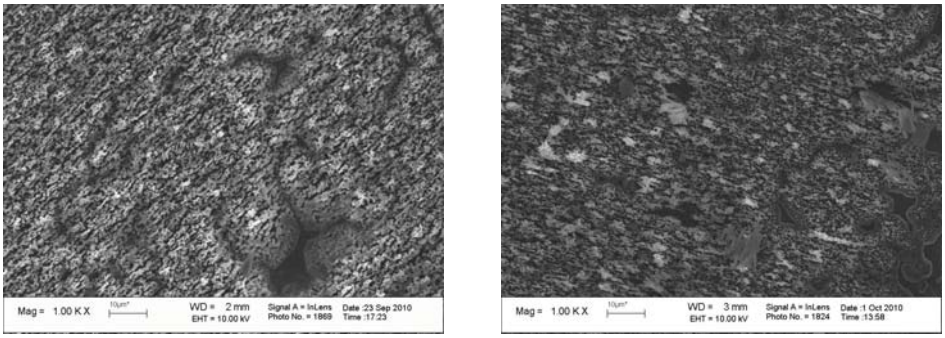

(a) With nucleation (b) Without nucleation

Figure 4: Comparison of deposition with and without nucleation pulse, deposited with a pulsed current of -5 mA (0.2 s)/0 A (2 s)

nanorods compared to the number of holes in the membrane. One possibility for this behavior is that in the deposition step, new holes are being formed (etched) in the membrane, leading to the formation of new nanorods. This assumption is based upon an experiment where the PC membrane was placed in the ionic liquid and left for 2 months, after which no sign of deterioration was visible in SEM. Hence, any etching process must occur as a result of the electrodeposition.

In an attempt to test this theory a series of experiments were performed where a commercial PC film, without pores as well as an in-house made film with a few pores, were used as membranes. In Figure 5, it is seen that when deposition was performed with a nonporous PC film, nevertheless nucleations were present on the surface. In this experiment the ionic liquid was dripped on the aluminium sample before placing the PC film on top of it, thus there was a supply of $Al_2Cl_7^-$ ions in close proximity to the sample during the deposition. One could argue that the nucleation was merely a result of plating, which was independent of the presence of the PC film and furthermore that no etching hence was necessary. On this basis, further studies were performed in which PC films with a few holes were used.

This was facilitated by using FiB (focused ion beam) induced pores in the same type of commercial PC film. By milling a cluster of 5 holes in a circular order, the growth mechanism could be studied. Since this membrane was made with a limited number of pores, an increase in the number of nanorods compared to the holes would confirm the hypothesis behind the growth mechanism. To eliminate the possibility of ionic liquid directly reaching the sample, it was added after the PC film was attached to the aluminium sample, forcing the liquid to go through the pores to reach the sample. Nevertheless, homogeneous nucleations across the entire sample was achieved as can be seen in Figure 6.

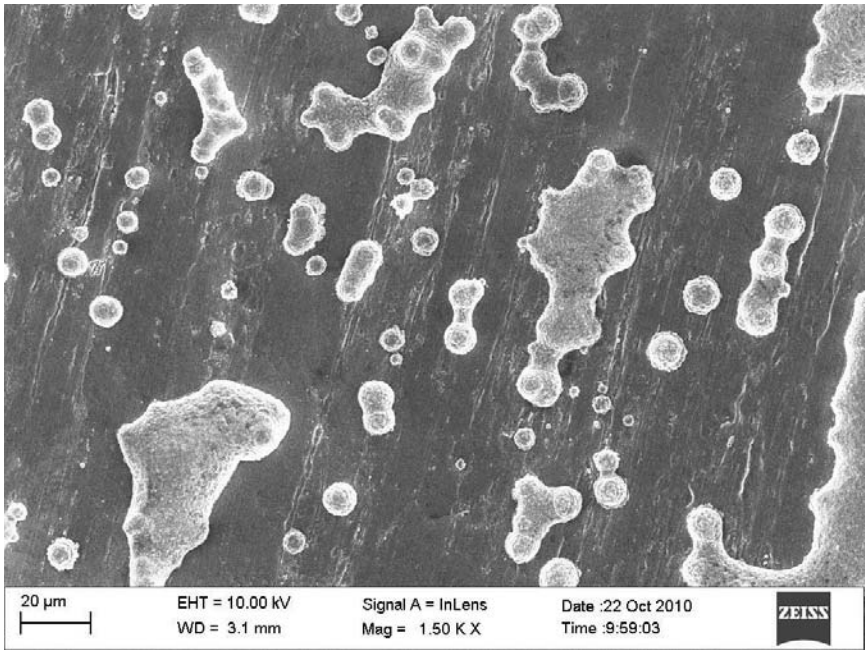

Figure 5: Nucleations in the deposition with a PC film without pores, deposited with a pulsed current of -5 mA (0.2 s)/0 A (2 s)

No clear matching between the rods and the associated pores could be made, subsequently no verification of the growth mechanism hypothesis could be established. As the FiB induced holes have a larger diameter than those of the commercial membrane ($\approx 2\ \mu m$ compared to 200 nm), the growth mechanism might be different. Consequently, in order to mimic the original porous PC membrane, the next step would be to use a commercial PC membrane with the same pore size but with a substantionally lower pore density.

4.1.2 Proposed nanorod growth mechanism

The template assisted nanorod deposition rests upon the hypothesis that for each nanorod there is an accompanied membrane hole, which allows for a high aspect ratio rod forming. Based upon this hypothesis, a comparison of SEM images of the PC membrane and the as-deposited aluminium nanorod samples should result in a 1:1 ratio between membrane holes and nanorods deposited. Nevertheless, a clear excess of nanorods in comparison with the obtained holes was occurent. Consequently, a new hypothesis is needed for the nanorod deposition with a PC membrane.

The founding assumption for a new hypothesis is that for every nanorod there has to be a hole in the PC membrane. Since the pore density is lower than the nanorod density, a logical assumption is that new pores are formed

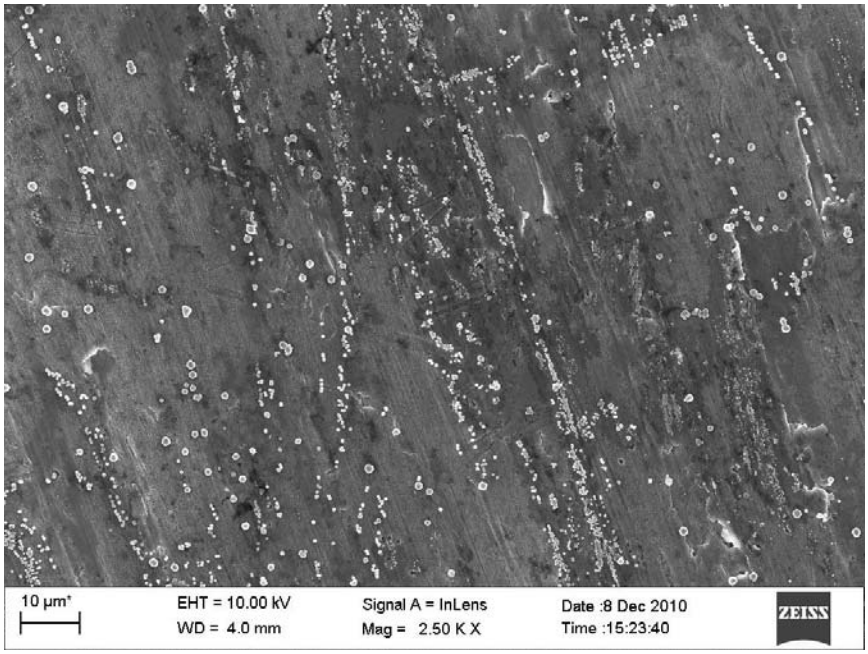

Figure 6: Homogeneous nucleation on aluminium sample in the PC film with pores experiment, deposited with a pulsed current of -5 mA (0.2 s)/0 A (2 s)

during the electrodeposition. Consequently, an etching process of the PC membrane must occur during the deposition. This leads to the following hypothesis, as illustrated in Figure 7.

Before deposition, the ionic liquid moves through the pores separating the PC membrane from the aluminium substrate. The first step of the electrodeposition is aluminium plating until the aluminium layer reaches the membrane. Since there is no room for additional plating on the entire surface, the nanorod growth is initiated, supported by the pore structure. The reduction of aluminium ions (see equation 1) in close vicinity of the polycarbonate membrane may lead to an etching of the membrane. A generation of the $Al_2Cl_7^-$ Lewis acid in the deposition process facilitates a corrosive environment leading to etching of the membrane. Since the nanorods are cylindrical, the etching would be radial leading to a widening of the initial pore. This widening of the pore may enable new nucleation, and furthermore new nanorods to be formed. However, since there is a local drop in the $Al_2Cl_7^-$ concentration near the first nanorod, the new rods may be formed along the membrane wall which enables structural support and more importantly a higher ion concentration. The new nanorods will in turn lead to a local increase in $Al_2Cl_7^-$ concentration which consequently leads to a radial etching of the membrane.

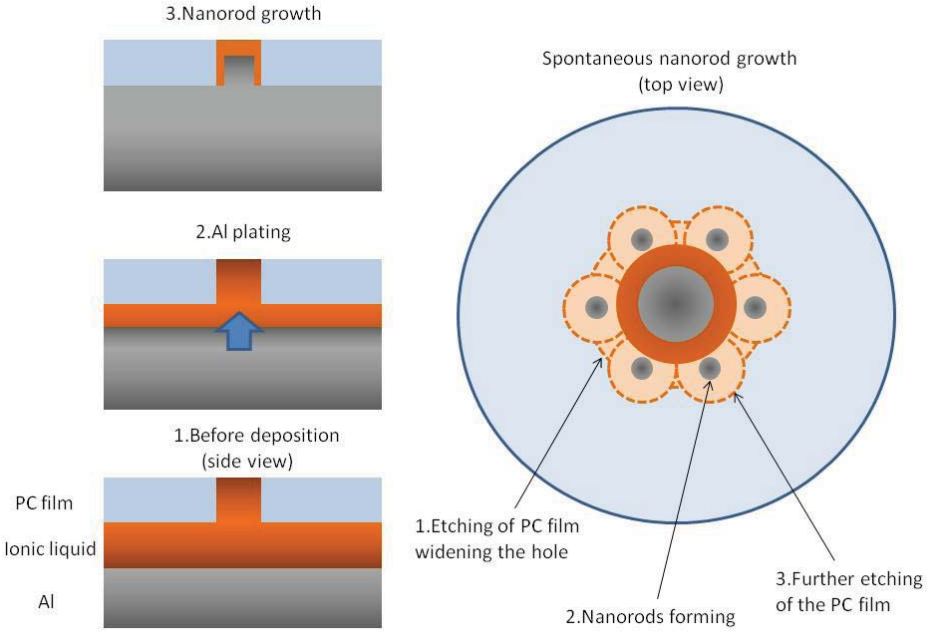

Figure 7: Aluminium nanorod growth mechanism

4.2 Vanadium oxide electrode material

Prestudies on the electrochemical properties of the vanadium oxide deposition revealed that oxidative galvanostatic deposition was possible with a current density of 1 mA/cm^2. A higher current lead to evolution of oxygen via oxidation of water. Cyclic voltammetry performed on the electrolyte (0.1 M $VOSO_4$), revealed an oxidation peak for V^{4+} to V^{5+} starting at 0.7 V (vs Ag/AgCl). The reaction was either carried out in one or two consequential oxidation steps, depending on the pH value of the electrolyte. The reactions are depicted in equations 7, 8 and 9 [27].

For pH$<$ 1.8

$$\begin{aligned} VO^{2+} + H_2O &\rightarrow VO_2^+ + 2H^+ + e^- \\ 2VO_2^+ + H_2O &\rightarrow V_2O_5 + 2H^+ \end{aligned} \tag{7}$$

For pH = 1.8

$$2VO^{2+} + 3H_2O \rightarrow V_2O_5 + 6H^+ + 2e^- \tag{8}$$

For pH$>$ 1.8

$$\begin{aligned} 10VO^{2+} + 18H_2O &\rightarrow H_2V_{10}O_{28}^{4-} + 34H^+ + 10e^- \\ H_2V_{10}O_{28}^{4-} + 4H^+ &\rightarrow 5V_2O_5 + 3H_2O \end{aligned} \tag{9}$$

Analyses of the thin film with both EDS and XRD were inconclusive leading to further analysis by XPS. This method however clearly showed that there was no vanadium oxide on the surface, furthermore the result pointed towards the presence of aluminium oxide. Which can be explained by the native oxide that forms when aluminium comes in contact with the atmospheric oxygen. This result could not be verified by XRD or EDS since the native aluminium oxide layer is too thin to detect. The XPS results are described in Table 1. The detection of nitrogen, fluorine and carbon are common in XPS analysis as they are present in the atmosphere and adhere well to most surfaces.

Element	Al(2p)	C(1s)	S(2p)	N(1s)	V(2p)	O(1s)	F(1s)
Atomic concentration	13.54	29.86	5.75	3.28	0.19	44.86	2.53

Table 1: XPS analysis of the V2O5 sample

4.2.1 pH dependence of V_2O_5 deposition

The electrodeposition was carried out at pH 1.8 and with a current density of 1 mA/cm^2. These parameters were selected to enable a deposition of V_2O_5. However since there is corrosion of aluminium in that region, the corroded aluminium could detach together with the attached vanadium oxide, leading to a failed attempt to deposit the wanted vanadium oxide. By comparing the Pourbaix diagrams for the vanadium and aluminium aqueous systems, Figure 8, a possible deposition range would be between pH 1.8-4. V_2O_5 deposition is possible at lower pH, however in this region aluminium undergoes corrosion and the deposition would not be favored. Even though aluminium corrodes in this region, deposition could be possible if the deposition rate is faster than the corrosion rate and a full coverage of the surface is reached before the corrosion is engaged.

As can be seen in Figure 8b, at pH 3-4 and with a potential below 0.2, VO_2 can be agglomerated leading to a reduced concentration of vanadium ions. By making a new batch of $VOSO_4$ electrolyte before every deposition, this problem could be addressed. However at pH above 3.8, a distinct color change was noted and a clear precipitate was visible on the bottom of the beaker.

Further studies of the pH dependence of V_2O_5 deposition were carried out at different pH values within the pH range of 2-4. Analysis was performed by gracing incidence X-ray diffraction in which the low incoming angle allows a surface specialized analysis. The diffractograms illustrated in Figure 9 clearly show an aluminium peak at the surface, meaning that the deposition was unsuccessful. This result was valid for the entire pH range leading to the conclusion that deposition of vanadium oxide on an

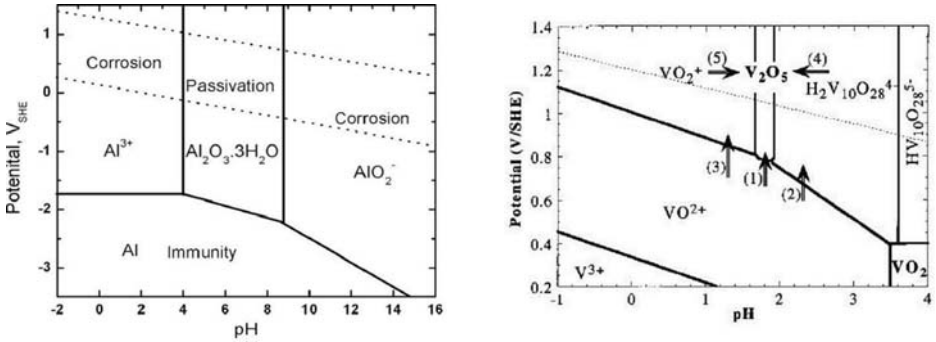

(a) Aluminium [29] (b) Vanadium [27]

Figure 8: Pourbaix diagram for vanadium and aluminium species in an aqueous solution

aluminium substrate is difficult without a stable protective layer on the aluminium. In the diffractogram of pH 2 a few small peaks are noticeable that are not corresponding to the aluminium phase. These peaks were matched to Al_2O_3 which would suggest a possibility of vanadium oxide deposition, however no vanadium oxide phase was detected.

In an attempt to tackle the corrosion problem of aluminium, a stainless steel sample was used as the substrate and the same galvanostatic deposition with a 1 mA current was performed.

Gracing incidence X-ray diffraction analysis was carried out on the sample and the results are illustrated in Figure 10. Even in this case the deposition was unsuccessful and the reaction most likely included an oxidation of the surface chromium which would explain the low potential during the deposition (in the range of 0.2-0.3 V).

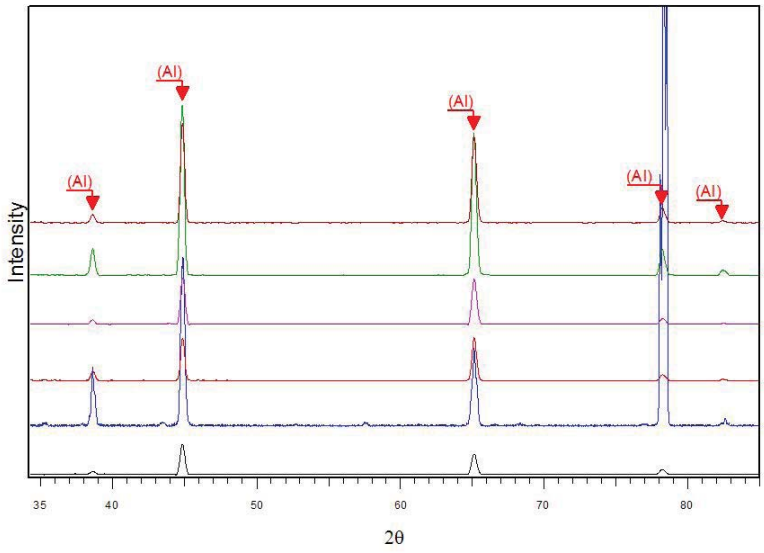

Figure 9: XRD analysis of the pH dependence of vanadium oxide deposition. From bottom and up; aluminium reference sample(black), pH 2(blue), pH 2.5(red), pH 3(purple), pH 3.5(green), pH 4(dark red). The red peaks correspond to aluminium (cubic).

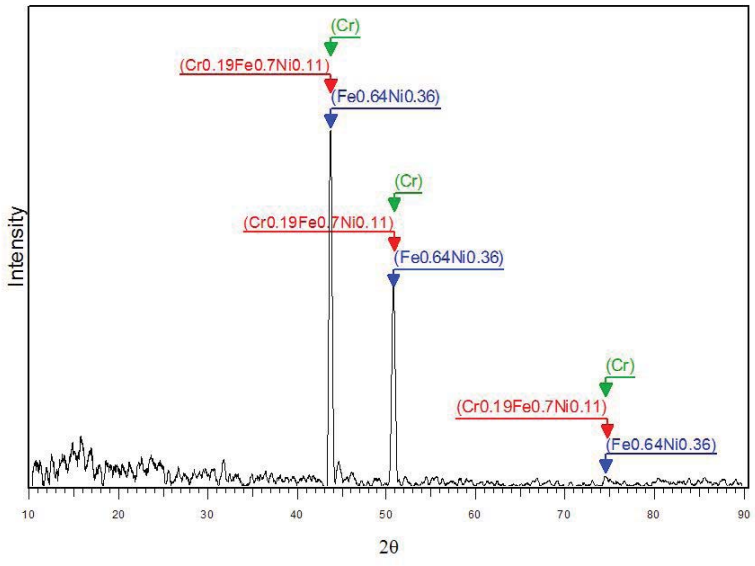

Figure 10: XRD analysis of vanadium oxide deposition on a stainless steel sample. Possible phases are: Iron Nickel ($Fe_{0.64}Ni_{0.36}$)(blue), Chromium Iron Nickel ($Cr_{0.19}Fe_{0.7}Ni_{0.11}$)(red), Chromium (Cr)(green).

5 Conclusions

Synthesis of a nanostructured aluminium current collector is possible with template assisted electrodeposition technique. By using a nucleation pulse prior to the deposition, the growth rate and aspect ratio of the nanorods were improved. Furthermore, a pulsed galvanostatic deposition technique was verified as an applicable method of growing nanorods, due to the improved ion diffusion during the rest pulse. The PC membrane showed interesting properties with regards to its use in electrodeposition of aluminium. The density of nanorods deposited with a nonhomogeneously ordered PC membrane, bears close resemblance to the nanorod density of a deposition with an ordered porous alumina membrane.

The surplus of nanorods in reference to the number of original pores bears close resemblance to the density nanorods acquired from deposition in a porous alumina membrane.

The hypothesis behind the nanorod growth mechanism formulated in this thesis is based upon the assumption that for each nanorod grown, an accompanied membrane pore is present. This leads to the hypothesis that for each new nanorod formed, an etching of the membrane occurs enabling a new rod to grow in the widened pore. Since the membrane is inert in the ionic liquid, the etching process must be initiated by the electrodeposition. Without any convincing results, a continued assumption is that a byproduct of the electrodeposition might be the etching reason. Whatever the mechanism might be, this new found nanorod growth is an astonishing discovery and further research should be carried out to investigate this further.

The electrodeposition of a vanadium oxide layer on top of the aluminium current collector is the final step in creating a 3-D cathode electrode. Following the work of Potiron *et al.* [27], who focused on depositing V_2O_5 on a platinum thin film, similar results were expected on our aluminium sample. Unfortunately the deposition was unsuccessful, most likely due to the instability of the protecting aluminium oxide in that region of the Pourbaix diagram seen in Figure 8a. The instability of the aluminium oxide in combination with the anodic current, allow for an oxidation of the underlying aluminium bulk material. As the bulk is oxidized it will dissolve into the electrolyte leading to a deterioration of the surface making deposition of a coating oxide difficult. In order to successfully deposit a coating oxide on the aluminium substrate, the deposition speed of the coating V_2O_5 must be higher than the aluminium corrosion rate. In order to have an inert aluminium oxide layer present, the pH must be above 4. However, as the pH is increased a precipitation of VO_2 is visible at pH 3.8. Though the aluminium oxide is unstable in the pH region of 1.8-4, the deterioration of the oxide is not instantaneous making deposition possible in theory, if the vanadium oxide deposition speed is high enough to grow at least one monolayer on the substrate. A full V_2O_5 coating would protect the substrate from further alu-

minium corrosion and the oxide would then be able to grow. This assumes that the aluminium diffusion speed low enough compared to the growth rate of the vanadium oxide.

In addition to the aluminium corrosion, a limiting factor for the V_2O_5 deposition lies in the usage of a constant current. Since the current will follow the path of least resistance, the reaction which has the lowest potential will consequently be the one receiving the current. The pH region used in the deposition enables deterioration of the passivating aluminium oxide, which further enable aluminium corrosion to occur and consequently dominate the constant current. Meaning, the deposition of vanadium oxide is not only limited by the deterioration of the protective aluminium oxide but also by the lack of a constant current. One possibility would be to use a constant potential instead of a constant current. However following the same logic as for the galvanostatic deposition, the same aluminium domination of the potential would most likely be seen due to the fact that aluminium oxidation has a very low standard potential.

In conclusion, synthesis of a nanostructured aluminium current collector by template assisted electrodeposition is an applicable method. Furthermore, the polycarbonate membrane shows interesting qualities and is anticipated to be a useful material for low cost synthesis of current collectors. The continued deposition of a Li-ion host material on aluminium is problematic and continued research is required to solve the problems with the stability of the protective Al_2O_3 layer.

6 Future prospects

The PC membrane electrodeposition of aluminium nanorods requires continued research to verify the mechanism of the nanorod growth. As described in section 4.1.1, by continuing the work with a similar PC membrane (with a lower pore density), some clarity might be obtained. The focus should be on trying to mimic the original membrane but with a lower pore density, as to be able to follow the nanorod growth from a limited amount of pores and see how the rods grow.

Deposition of a cathode material on the aluminium current collector needs substantionally more work not only to find a possible deposition technique but to investigate the electrochemical properties of a half-cell and finally a complete battery cell. Measurements of the electrolyte after deposition with inductively coupled plasma (ICP), would reveal if an aluminium residue is present in the solution. This analysis should be performed in order to substantiate the hypothesis that aluminium corrodes during the electrodeposition and thus might be the reason for the failed precipitation of V_2O_5. Potentiostatic electrodeposition shows little promise in theory, but nonetheless the experiment should be performed. A promising route is to use another cathode material as a buffer in the deposition. One possibility is to use a cathode material which can be oxidized in a pH-potential region that aluminium is stable in. The new cathode material will then protect the aluminium as the deposition of V_2O_5 is performed, assuming that the buffer cathode material is stable in at the low pH of the vanadylsulphate electrolyte. A possible candidate is MnO_x.

7 Acknowledgments

First and foremost I want to express great appreciation towards my main supervisor Prof. Leif Nyholm for his continuous advise and guidance. I would also like to acknowledge his uncanning ability to turn the most hopeless results into excellent ones, in a way that only Leif can.

Furthermore, I would like to thank my practical supervisor Gabriel Oltean, as he was my Obi wan in the jungle of electrochemistry. His foundation enabled my research to take off to a swift and successful start and I appreciate our good collaboration.

I would also like to express my gratitude towards Prof. Kristina Edström and Fredrik Björefors for many fruitful discussions and insight into the outside world of batteries.

Much appreciation goes out to my advisor Torbjörn Gustafsson, your knowledge and assistance played great part especially in the vanadium section of my thesis work. A social acknowledgment goes out to my partners in crime, Jonas and Sara. Your support made this thesis work a very pleasant experience and I will never forget our zero breaks. Special thanks goes out to my friend Linus who introduced me to the wonderful and all so challenging program that is LaTeX. Finally I would like to acknowledge the fun and warm group of people that is this institutions PhD workers.

8 References

[1] J.M. Tarascon, M. Armand, Issues and challenges facing rechargeable lithium batteries, *Nature*, 414(2001).

[2] D. Linden, T.B. Reddy, *Handbook of batteries*, 3rd edition, McGraw-Hill, New York, (2002) 35.1.

[3] P.G. Bruce, B. Scrosati, J-M. Tarascon, Nanomaterials for Rechargeable Lithium Batteries, *Angewandte Chemie*, 47(2008), 2930-2946.

[4] J.B. Goodenough, Y. Kim, Challenges for Rechargeable Li Batteries, *Chemistry of Materials*, 22(2010), 587-603.

[5] H. Bryngelsson, J. Eskhult, L. Nyholm, K. Edström, Thin films of Cu_2Sb and Cu_9Sb_2 as anode materials in Li-ion batteries, *Electrochimica Acta*, 53(2008), 7226-7234.

[6] J.W. Long, B. Dunn, D.R. Rolison, H.S. White, Three-Dimensional Battery Architectures, *Chemical Reviews*, 104(2004), 4463-4492.

[7] X. Huang, X. Li, H. Wang, Z. Pan, M. Qu, Z. Yu, Synthesis and electrochemical performance of Li2FeSiO4/C as cathode material for lithium batteries, *Solid State Ionics*, 181(2010), 1451-1455.

[8] A.S. Arico, P. Bruce, B. Scrosati, J.-M. Tarascon, W. Van Schalkwijc, Nanostructured materials for advanced energy conversion and storage devices, *Nature Materials* 2005, 4, 366.

[9] D. Golodnitsky, M. Nathan, V. Yufit, E. Strauss, K. Freedman, L. Burstein, A. Gladkich, E. Peled, Progress in three-dimensional (3D) Li-ion microbatteries, *Solid State Ionics* 177(2006), 28112819.

[10] P.L Taberna, S. Mitra , P. Poizot , P. Simon , J-M. Tarascon, High rate capabilities Fe_3O_4-based Cu nano-architectured electrodes for lithium-ion battery applications, *Nature Materials*, 5(2006) 567-573.

[11] G. Cao, D. Liu, Template-based synthesis of nanorod, nanowire, and nanotube arrays, *Advances in Colloid and Interface Science*, 136 (2008), 4564.

[12] A. Keilbach, J. Moses, R. Köhn, M. Döblinger, T. Bein, Electrodeposition of Copper and Silver nanowires in Hierarchical mesoporous Silica/Anodic Alumina nanostructures, *Chemistry of Materials*, 22(2010), 5430-5436.

[13] L. Soleimany, A. Dolati, M. Ghorbani, A study on the kinetics of gold nanowire electrodeposition in polycarbonate templates, *Journal of Electroanalytical Chemistry*, 645(2010), 28-34.

[14] A. Azarian, A. Iraj zad, A. Dolati, S. M. Mahdavi, Field emission of Co nanowires in polycarbonate template, *Thin Solid Films*, 517(2009), 1736-1739.

[15] Y. Konoshi, M. Motoyama, H. Matsushima, Y. Fukunaka, R. Ishii, Y. Ito, Electrodeposition of Cu nanowire arrays with a template, *Journal of Electroanalytical Chemistry*, 559(2003), 149-153.

[16] E. Perre, L. Nyholm, T. Gustafsson, P-L. Taberna, P. Simon, K. Edström, Direct electrodeposition of aluminium nano-rods, *Electrochemistry Communications*, 10(2008), 1467-1470.

[17] P. L. Taberna, S. Mitra, P. Poizot, P. Simon, J. Tarascon, High rate capabilities Fe_3O_4-based Cu nano-architectured electrodes for lithium-ion battery applications, *Nature Materials*, 5(2006), 567-573.

[18] C. Lecoeur, J-M. Tarascon, C. Guery, Al current collectors for Li-ion batteries made via a template-free electrodeposition process in ionic liquids, *Journal of the Electrochemical Society*, 157(2010), A641-A646.

[19] T. Jiang, M. J. Chollier Brym, G. Dub, A. Lasia, G. M. Brisard, Electrodeposition of aluminium from ionic liquids: Part 1-electrodeposition and surface morphology of aluminium from aluminium chloride ($AlCl_3$)-1-ethyl-3-methylimidazolium chloride ([EMIm]Cl) ionic liquids, *Surface and Coatings Technology*, 201(2006), 1-9.

[20] F.F.C. Bazito, R.M. Torresi, Cathodes for lithium ion batteries: The benefits of using nanostructured materials, *Journal of Brazilian Chemical Society*, 4(2006), 627-642.

[21] J.W. Fergus, Recent developments in cathode materials for lithium ion batteries, *Journal of Power sources*, 195(2010), 939-954

[22] Y-H. Huang, K-S. Park, J.B. Goodenough, Improving lithium batteries by tethering carbon-coated $LiFePO_4$ to polypyrrole, *Journal of The Electrochemical Society*, 153(2006), A2282-A2286.

[23] E. Shembel, R. Apostolova, V. Nagirny, D. Aurbach, B. Markovsky, Synthesis, investigation and practical application in lithium batteries of some compounds based on vanadium oxides, *Journal of Power Sources*, 80(1999), 90-97.

[24] N. Ding, X. Feng, S. Liu, J. Xiu, X. Fang, I. Lieberwirth, C. Chen, High capacity and excellent cyclability of vanadium (IV) oxide in lithium

battery applications, *Electrochemistry Communications*, 11(2009), 538-541.

[25] I-H. Kim, J-H. Kim, B-W. Cho, Y-H. Lee, K-B. Kim, Synthesis and electrochemical characterization of vanadium oxide on carbon nanotube film substrate for pseudocapacitor applications, *Journal of The Electrochemical Society*, 153(2006), A989-A996.

[26] G. Oltean, L. Nyholm, K. Edström, Galvanostatic electrodeposition of aluminium nano-rods for Li-ion 3D micro-battery current collectors, *Electrochimica Acta*, in press.

[27] E. Potiron, A. Le Gal La Salle, A. Verbaere, Y. Piffard, D. Guyomard, Electrochemically synthesized vanadium oxide as lithium insertion hosts, *Electrochimica Acta*, 45(1999), 197-214.

[28] C.R. Brundle, C.A. Evans Jr., S. Wilson, Encyclopedia of Materials Characterization, *Surfaces Interfaces Thin Films*, (1992)

[29] J. Zhu, L.H. Hihara, Corrosion of continuous alumina-fibre reinforced Al-2 wt.% Cu-T6 metal-matrix composite in 3.15 wt.% NaCl solution, *Corrosion Science*, 52(2010), 406-415.